Stability of Straight Delamination Blisters

Basile Audoly

Laboratoire de Physique Statistique de l'École Normale Supérieure, 24 rue Lhomond, 75230 Paris Cedex 05, France

(Received 2 July 1999)

We consider the buckle-driven delamination of biaxially compressed thin films. Telephone-cord-like patterns observed in experiments are explained as a result of the buckling behavior of the film. We perform a stability analysis of a straight blister. A mechanism of instability causing undulations in an advancing finger of delamination is pointed out, which we claim to be the basic phenomenon explaining the zigzag pattern. We predict a transition to a varicose (unobserved as yet) pattern at low Poisson ratios.

PACS numbers: 68.55.–a, 46.32.+x

The elasticity of thin plates has been investigated by Föppl and von Kármán (FvK) early in this century. Because of the intricate nature of the equations, however, there remain many unsolved theoretical questions in this area. For example, thin films delamination is still poorly understood, although such films are widely used in the industry (e.g., insulating layers in microelectronics). A thin coated film is often obtained by vapor deposition on a substrate; if its thermal expansion coefficient is smaller than that of the substrate, the film acquires a residual biaxial compression upon cooling. In this case, a competition between this compression and the film-substrate cohesion can result in the partial delamination of the coating: in some region, the film lifts off the substrate, and forms a blister. Delamination patterns looking like telephone cords have been observed in a vast variety of films [1], and have recently been reproduced in computer simulations [2]. The configuration of the film in the delaminated region is an elongated tunnel with undulating edges, behind a propagating tip.

Although the first observations of telephone-cord-like patterns go back to the early 1960's [3], a satisfactory explanation for the origin of the undulations is still lacking. Recently, Gioia and Ortiz [4] have proposed a model capable of replicating the telephone-cord morphology; however, their approach neglects important, if not essential, aspects of thin film mechanics (in-plane displacements of the film are discarded), and does not explain the origin of the wrinkles. Yu *et al.* [5] have studied the telephone-cord-like patterns, overlooking the boundary conditions at the edge of the film, while these are known to be essential for the selection of the buckling patterns [6].

We explain these wrinkles from the mechanical properties of the film, and show that all aspects of thin film mechanics (in-plane displacements, lateral boundary conditions) are important for the understanding of these patterns. We start from the only elongated pattern that could receive an exact analytical treatment, the straight-sided blister [7], also called the "Euler column." When the Euler column is formed, the buckling of the film mostly releases the transversal stress. Prior to delamination, the initial compression of the film was biaxial and isotropic; a large longitudinal compression therefore remains present in the Euler column. We perform a linear stability analysis of the Euler column, taking into account this longitudinal compression. To do this, we use the FvK equations for the film. We find that, for relatively small values of the compression, the column becomes unstable, as it undergoes a secondary buckling in the longitudinal direction.

In the delaminated region, the shape of the thin film is found by solving the FvK equations for plates. Let $\zeta(x, y)$ be the vertical displacement of the film—for a simple description, we shall assume that the original plane (x, y) of the film is horizontal, gravity having no effect. The equations of mechanical equilibrium in the plane tangent to the film allow one to define the Airy potential, $\chi(x, y)$. The tangential components of the stress derive from it: $\sigma_{xx} = \partial_{yy}\chi$, $\sigma_{yy} = \partial_{xx}\chi$, $\sigma_{xy} = -\partial_{xy}\chi$. The FvK equations are two coupled nonlinear partial differential equations in ζ and χ [8]:

$$\Delta^2\chi + E\left[\frac{\partial^2\zeta}{\partial x^2}\frac{\partial^2\zeta}{\partial y^2} - \left(\frac{\partial^2\zeta}{\partial x\,\partial y}\right)^2\right] = 0, \quad (1a)$$

$$D\Delta^2\zeta + h\sigma_0\Delta\zeta - h\{\chi, \zeta\} = 0, \quad (1b)$$

where $\sigma_0 > 0$ is the initial biaxial compression of the film, $D = Eh^3/[12(1 - \nu^2)]$ its bending rigidity, E is the Young's modulus, ν is the Poisson ratio, h is the thickness of the film, and $\{\chi, \zeta\} = (\partial^2\chi/\partial y^2)(\partial^2\zeta/\partial x^2) + (\partial^2\chi/\partial x^2)(\partial^2\zeta/\partial y^2) - 2(\partial^2\chi/\partial x\,\partial y)(\partial^2\zeta/\partial x\,\partial y)$. The horizontal components of the displacement have been eliminated from these equations, but we shall need them to express boundary conditions later; they can be recovered from the following relations [8], which are compatible by (1a):

$$\frac{\partial u_x}{\partial x} = \frac{1}{E}\left(\frac{\partial^2\chi}{\partial y^2} - \nu\frac{\partial^2\chi}{\partial x^2}\right) - \frac{1}{2}\left(\frac{\partial\zeta}{\partial x}\right)^2, \quad (2a)$$

$$\frac{\partial u_y}{\partial y} = \frac{1}{E}\left(\frac{\partial^2\chi}{\partial x^2} - \nu\frac{\partial^2\chi}{\partial y^2}\right) - \frac{1}{2}\left(\frac{\partial\zeta}{\partial y}\right)^2, \quad (2b)$$

$$\frac{\partial u_x}{\partial y} + \frac{\partial u_y}{\partial x} = \frac{-2(1 + \nu)}{E}\frac{\partial^2\chi}{\partial x\,\partial y} - \frac{\partial\zeta}{\partial x}\frac{\partial\zeta}{\partial y}. \quad (2c)$$

 0031-9007/99/83(20)/4124(4)$15.00 © 1999 The American Physical Society

A solution of the FvK equations representing a straight-sided blister of width $2b$ is known; it is sketched in Fig. 1. It is found by solving the Eqs. (1), assuming cylindrical symmetry: $\partial_y \zeta = \partial_y \sigma_{\alpha\beta} = 0$. As the substrate is much thicker than the film, clamped boundary conditions must be imposed at the edge of the blister:

$$u_x = u_y = 0, \qquad \zeta = \zeta_x = 0 \quad \text{at } x = \pm b\,. \tag{3}$$

The conditions $u_x(\pm b, y) = u_y(\pm b, y) = 0$ are to be expressed using (2). If the initial compression is larger than the critical value $\sigma_c^E = (\pi^2 D)/(b^2 h)$, then there exists a buckled solution, the Euler column. It is defined by [7]:

$$\zeta^E(x, y) = \zeta_m^E \frac{1 + \cos\frac{\pi x}{b}}{2}, \qquad \zeta_m^E = \frac{2h}{\sqrt{3}} \left(\frac{\sigma_0}{\sigma_c^E} - 1\right)^{1/2}. \tag{4}$$

This solution has no Gaussian curvature, which makes the FvK equations linear [the second term in Eq. (1a) vanishes]. Nonlinearities arise due to the boundary conditions only. This explains that an analytical solution can be found.

The compression in the column is uniform, and has the value $\sigma_{xx} = -\sigma_c^E$, $\sigma_{yy} = -[(1 - \nu)\sigma_0 + \nu\,\sigma_c^E]$, $\sigma_{xy} = 0$. In comparison with the unbuckled state, all the components of the stress have decreased in magnitude. However, this buckling releases the initial biaxial compression in the transversal direction only: typical initial strains in the film can be as high as a few percent [9], so that compressions in the film may be far beyond the buckling threshold ($\sigma_0 \gg \sigma_c^E$). As a result, an appreciable longitudinal compression $\sigma_{yy} \approx -(1 - \nu)\sigma_0$ remains present in the film after the Euler buckling. This residual stress may induce a secondary buckling of the Euler column, addressed by studying the linear stability of the straight-sided blister.

Let $(\hat{\zeta}, \hat{\chi})$ be a small perturbation in the configuration of the film near the Euler solution (4). We use dimensionless variables: $\hat{\sigma}_0 = \sigma_0/\sigma_c^E$, $(\hat{x}, \hat{y}) = (x, y)/b$, $\hat{\zeta} = (\zeta - \zeta^E)/[b\,(\sigma_c^E/E)^{1/2}]$, $\hat{\chi} = (\chi - \chi^E)/[2\pi(1 - \nu^2)^{1/2}(\hat{\sigma}_0 - 1)^{1/2}\,\sigma_c^E/b^2)]$. The Euler column being invariant by translation, one considers perturbations $(\hat{\zeta}, \hat{\chi})$ that are harmonic in the y direction. Let l be the longitudinal wavelength, $\hat{l} = l/b$, and $\hat{q} = 2\pi/\hat{l}$ the wave vector: $\hat{\chi}(\hat{x}, \hat{y}) = \hat{\chi}_{\hat{q}}(\hat{x})\cos(\hat{q}\hat{y})$, $\hat{\zeta}(\hat{x}, \hat{y}) = \hat{\zeta}_{\hat{q}}(\hat{x})\cos(\hat{q}\hat{y})$. For a mode of given wave vector, $\hat{q}$, the linearized Eqs. (1) yield two coupled ordinary linear differential equations of order 4 for $\zeta_{\hat{q}}(\hat{x})$ and $\chi_{\hat{q}}(\hat{x})$:

$$\chi_{\hat{q}}^{(4)}(\hat{x}) - 2\,\hat{q}^2 \chi_{\hat{q}}''(\hat{x}) + \hat{q}^4 \chi_{\hat{q}}(\hat{x}) + \hat{q}^2[4\pi^2(1 - \nu^2)(\hat{\sigma}_0 - 1)]\cos(\pi\hat{x})\zeta_{\hat{q}}(\hat{x}) = 0\,, \tag{5a}$$

$$-\hat{q}^2\cos(\pi\hat{x})\hat{\chi}_{\hat{q}}(\hat{x}) + 1/\pi^2 \zeta_{\hat{q}}^{(4)}(\hat{x}) + \frac{\pi^2 - 2\,\hat{q}^2}{\pi^2}\zeta_{\hat{q}}(\hat{x}) + \{\hat{q}^4/\pi^2 - \hat{q}^2[\nu + (1 - \nu)\hat{\sigma}_0]\}\zeta_{\hat{q}}(\hat{x}) = 0\,, \tag{5b}$$

where $f^{(n)} = d^n f/dx^n$. When linearized, Eqs. (3) expressed using Eqs. (2) yield eight boundary conditions:

$$\text{at } \hat{x} = \pm 1, \qquad \hat{\zeta}_{\hat{q}} = \hat{\zeta}_{\hat{q}}' = 0\,, \qquad \hat{\chi}_{\hat{q}}'' + \hat{q}^2\nu\hat{\chi}_{\hat{q}} + \hat{\chi}_{\hat{q}}^{(3)} - (2 + \nu)\hat{q}^2\hat{\chi}_{\hat{q}}' = 0\,. \tag{6}$$

Remarkably, any small parameter has been eliminated in Eqs. (5) and (6). Only ν and $\hat{\sigma}_0$ remain, which are both of order unity. This may look surprising at first: the mechanics of thin films and other elastic plates is ruled to a large extent by a small parameter, h/b in the present case. This small parameter makes the film much easier to bend than to stretch. The easy formation of local singularities in elastic films, such as d-cones [10] or ridges [11], follows from the smallness of this parameter. So, how could we get rid of this small number if it is so essential to the mechanics of thin films? The answer is that, in contrast to recent works on elastic plates, we are considering a thin film submitted to tangential stretching (along the edge of the blister, the longitudinal compression $\sigma_0 \neq 0$ is transmitted to the film). As a result, the extensional contribution to the elastic energy is always present (the instability investigated below results from a competition between bending and stretching).

A shooting method can be used to isolate numerically the solutions of Eqs. (5) satisfying the boundary conditions (6). They correspond to the marginally stable configurations of the Euler column. For each value of ν, this yields the diagram of linear stability of the Euler column in the $(\hat{l}, \hat{\sigma}_0)$ plane, as in Fig. 2. The superscript "S" stands for "secondary" buckling. Because the Euler column is symmetric under $x \leftrightarrow (-x)$, the marginal modes that are symmetric, or antisymmetric in the x direction, have been sought independently; hence, the two branches, $S+$ (symmetric) and $S-$ (antisymmetric), on the diagram.

For every value of ν, the most unstable symmetric and antisymmetric mode can be located on the diagram: let $\sigma_c^{S\pm}(\nu)$ and $l^{S\pm}(\nu)$ be the corresponding critical initial compression, and wavelength. In Fig. 3, these quantities have been plotted versus ν. For $\sigma_0 > \sigma_c^{S\pm}(\nu)$, the Euler column buckles under the residual longitudinal

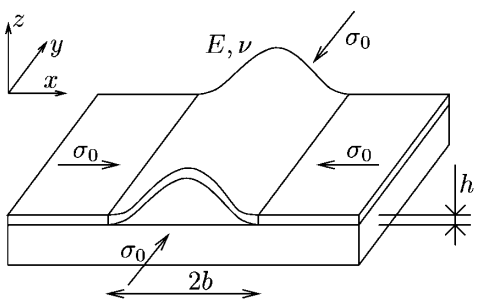

FIG. 1. The Euler column, solution of the FvK equations above the critical initial compression $\sigma_0 > \sigma_c^E$.

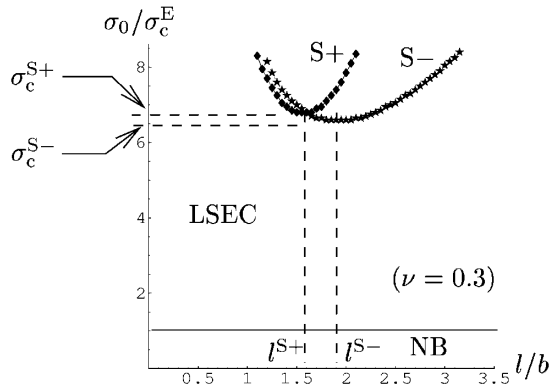

FIG. 2. Diagram of linear stability of the Euler column: no buckling (NB), linearly stable Euler column (LSEC), unstable Euler column by secondary antisymmetric buckling ($S-$), or secondary symmetric buckling ($S+$).

compression. Typically, the dimensionless buckling parameter (σ_0/σ_c^E) lies in the range 25–75 in experiments. This estimate has been obtained from Eq. (4), using values of $h \sim 200$ nm and $\zeta_m^E \sim 1.5$ μm provided in Ref. [9]. Comparison with $\sigma_c^S/\sigma_c^E \approx 6.5$ in Fig. 3 shows that the Euler column in unstable under typical experimental conditions; this explains why straight tunnels are very seldom observed.

For $\nu < \nu_c$, the most unstable mode is symmetric, while for $\nu > \nu_c$ it is antisymmetric. The number ν_c can be determined numerically as the value at which the curves $\sigma_c^{S+}(\nu)$ and $\sigma_c^{S-}(\nu)$ intersect in Fig. 3. As these curves do not depend on any parameter other than ν, its value is universal: $\nu_c = 0.255 \pm 0.001$. The configuration of the film after longitudinal buckling is represented in Fig. 4. The symmetric buckling ($S+$) involves vertical undulations of the Euler column, while the antisymmetric one ($S-$) looks more like a transverse periodic deformation of the column. The selection of the

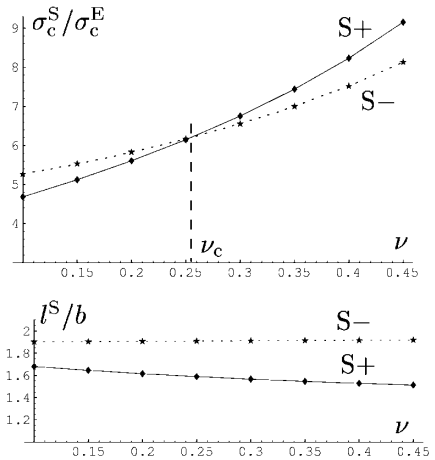

FIG. 3. Critical compression, σ_c^S, and wavelength, l^S, of the mode destabilizing the Euler column, by symmetric ($S+$) or antisymmetric ($S-$) secondary buckling. Dependence on the Poisson ratio of the film, ν is plotted.

symmetric versus antisymmetric pattern is understood as follows. The density of stretching elastic energy in a plate [8],

$$\mathcal{E}_s = \frac{E}{1-\nu^2}\left[u_{xx}^2 + u_{yy}^2 + 2\nu u_{xx}u_{yy} + 2(1-\nu)\,u_{xy}^2\right],$$

shows that the relative energetic cost of shear (u_{xy} term) versus compression (u_{xx} and u_{yy} terms) increases as ν decreases. This explains that the symmetric secondary buckling, which involves less shear than the antisymmetric one, is obtained at lower values of ν.

So far, the blister had imposed fixed, straight edges, and advance of the crack between film and substrate has not been discussed. In this paragraph, we consider the lateral growth of the preexisting, infinitely long, Euler column. As long as the edges of the blister remain straight and parallel, the spread of this column can be easily incorporated in the preceding analysis. The prediction of the width of the column, b, as a function of the initial compression, σ_0, relies on a propagation criterion for the interface crack, and is not discussed in this Letter; we shall merely mention that cracking a unit area of the interface in mode II (shearing) requires more energy than in mode I (opening), a fact which seems essential to explain the stability of the column [12,13]. The only effect of the increase of b is to lower progressively $\sigma_c^E \propto b^{-2}$. As shown above, the ratio σ_c^S/σ_c^E depends only on ν and not on b, so that

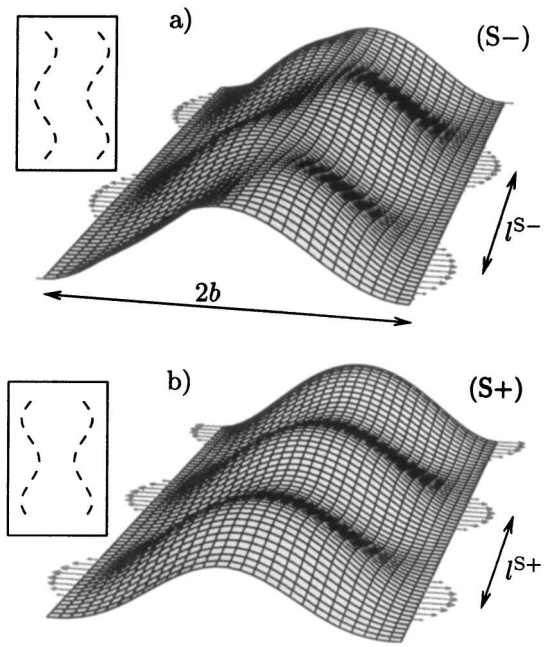

FIG. 4. Secondary buckling of the Euler column under the effect of the residual longitudinal compression (amplitude of the deflection is arbitrary). When (a) $\nu = 0.3$ the most unstable mode is antisymmetric ($S-$), while (b) for $\nu = 0.2$, it is symmetric ($S+$). Instability of the delamination front caused by this secondary buckling has been represented by the lateral arrows, leading to delamination patterns in the insets.

$\sigma_c^S \propto b^{-2}$ also decreases. For a given initial compression σ_0, there exists a critical width of the column where σ_c^S becomes smaller than σ_0, and the column buckles longitudinally. The loading on the delamination front is then no longer uniform. As shown in Fig. 4, portions of the delamination front become unstable: lateral arrows have been drawn, with a length proportional to the increase of G caused by the secondary buckling, where G is the energy release rate [14] along the film-substrate crack. Above this critical width, the sides of the blister cannot remain straight, and a tunnel with wavy edges is formed. The symmetry of the marginal modes suggests that these edges remain parallel if $\nu > \nu_c$, and are mirror symmetric if $\nu < \nu_c$, as shown in the insets. The increase of σ_0 has exactly the same effects as that of b, as the dimensionless buckling parameter has the form $\sigma_0/\sigma_c^S \propto \sigma_0 b^2$. Destabilization of the Euler column can result from the lateral growth of the column (increase of b), from the increase of σ_0, or both. This picture is strongly supported by an experimental observation: when a sample with a preexisting, infinite, *straight-sided* blister is cooled down, the straight edges become unstable, leading to a telephone-cord-like morphology [15] (the cooling increases σ_0).

In most experiments, telephone-cord blisters do not result from the destabilization of a preexisting, infinite, straight blister: they wave as they spread forward. The advance of a finger of delamination is a very difficult problem, because solutions to the FvK equations are not available, except for very simple geometries of the boundary, and the edge of the blister is not even known in advance. However, the results derived above suggest a simple mechanism of instability affecting the propagation of a semi-infinite finger of delamination, leading to undulations; by finger, we mean an elongated, straight blister. Consider a film with a Poisson ratio $\nu > \nu_c$ (for most films used in experiments, ν is very close to 0.3, which is indeed larger than ν_c). For typical experimental widths of blisters and initial compressions, $\sigma_0 \gg \sigma_c^E$, as noted above. Therefore, the portion of the blister well behind the tip is a Euler column which shall undergo an antisymmetric longitudinal buckling. The undulations are transmitted to the tip via the elasticity of the film. The $x \leftrightarrow (-x)$ symmetry at the tip is broken, which prevents straight propagation (see Fig. 5). This generically leads to undulations in the path of the blister [16]. This approach suggests that the wavelength of the pattern shall be close to the natural longitudinal length scale, $l^{S-} \approx 1.9b$. In experiments, the width, $2b$, and the wavelength of the telephone cords are indeed comparable [1].

In conclusion, the present approach demonstrates that the undulations in the patterns of delamination permit an optimal release of the elastic energy stored in the film. This interpretation simply relies on the elastic properties of the film, which is consistent with the fact that these patterns have been observed in a variety of experimental conditions. Analytical investigations are limited to a weakly nonlinear regime ($\sigma_0 \sim \sigma_c^S$), while experimental blisters are in fact in a fully nonlinear regime ($\sigma_0 \gg \sigma_c^S$). The value of ν_c, which selects the antisymmetric, versus symmetric, pattern shall be affected. Experiments using macroscopic plates are being conducted to explore this fully nonlinear regime.

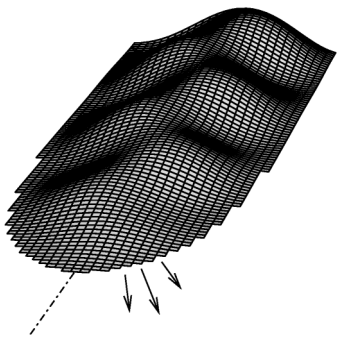

FIG. 5. A mechanism of instability leading to undulations in a finger of delamination: longitudinal buckling in the tail of the blister breaks the symmetry at the tip, and favors oblique propagation.

The Laboratoire de Physique Statistique is associé with the CNRS, the École Normale Supérieure, and the Universités Paris VI and Paris VII.

[1] For a review and many micrographs, see Ref. [4].
[2] K. M. Crosby and R. M. Bradley, Phys. Rev. E **59**, R2542 (1999).
[3] See, e.g., J. R. Priest *et al., Transactions of the Ninth National Symposium of the American Vacuum Society,* edited by G. H. Bancroft (Macmillan, New York, 1962), pp. 121–124.
[4] G. Gioia and M. Ortiz, Adv. Appl. Mech. **33**, 119 (1997).
[5] H. Y. Yu, C. Kim, and S. C. Sanday, Thin Solid Films **196**, 229 (1991).
[6] M. Boucif, J. E. Wesfreid, and E. Guyon, Eur. J. Mech. A, Solids **10**, 641 (1991).
[7] J. W. Hutchinson and Z. Suo, Adv. Appl. Mech. **29**, 63 (1991).
[8] L. D. Landau and E. M. Lifschitz, *Theory of Elasticity* (Pergamon, New York, 1959).
[9] G. Gille and B. Rau, Thins Solid Films **120**, 109 (1984).
[10] M. Ben Amar and Y. Pomeau, Proc. R. Soc. London A **453**, 729 (1997).
[11] A. E. Lobkovsky, Phys. Rev. E **53**, 3750 (1996); E. M. Kramer and T. A. Witten, Phys. Rev. Lett. **78**, 1303 (1997).
[12] J. W. Hutchinson, M. D. Thouless, and E. G. Liniger, Acta Metall. Mater. **40**, 295 (1992).
[13] B. Audoly (to be published).
[14] J. R. Rice, J. Appl. Mech. **35**, 379 (1968).
[15] M. D. Thouless (private communication).
[16] M. Adda-Bedia and Y. Pomeau, Phys. Rev. E **52**, 4105 (1995).